Available online at www.sciencedirect.com

ScienceDirect

Mendeleev Commun., 2023, **33**, 676–678

Mendeleev Communications

Properties of core–shell nanoparticles based on PLGA and human serum albumin prepared by different methods

Julia O. Kotova,*[a] Nadezhda S. Osipova,[a] Julia A. Malinovskaya,[a,b] Pavel A. Melnikov[b] and Svetlana E. Gelperina[a]

[a] *D. I. Mendeleev University of Chemical Technology of Russia, 125047 Moscow, Russian Federation. E-mail: juliakot1412@gmail.com*

[b] *V. P. Serbsky National Medical Research Centre of Psychiatry and Narcology, 119034 Moscow, Russian Federation*

DOI: 10.1016/j.mencom.2023.09.027

Core–shell nanoparticles with poly(lactide-*co*-glycolide) cores and human serum albumin shells (PLGA/HSA NPs) were prepared by three methods: by interfacial embedding of HSA in the PLGA NP surface during their formation and by adsorption or conjugation of HSA on pre-prepared PLGA NPs. All methods yielded PLGA/HSA NPs with a size of 130–150 nm and a narrow size distribution. *In vitro* fluorescence microscopy revealed the integrity of all core–shell systems when internalized in GL261 cells.

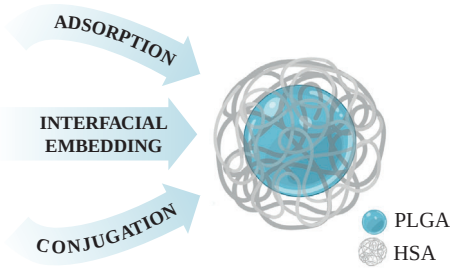

Keywords: core–shell nanoparticles, PLGA, human serum albumin, drug delivery systems, intracellular internalization, laser scanning confocal microscopy, LSCM.

Due to their biodegradability and biocompatibility, polylactic acid and especially its copolymers with glycolic acid (PLGA) are widely used for the preparation of drug delivery nanosystems.[1,2] However, like other colloidal particles, intravenously injected PLGA nanoparticles (PLGA NPs) tend to accumulate in macrophage-rich organs (*e.g.*, liver and spleen), making it difficult to deliver drugs to other targets.[3] This problem could be solved by conjugation of NPs with biovectors, molecules with high affinity for specific receptors expressed in the target organ. However, the modification of the PLGA NP surface with bioligands is difficult because the functional groups on the PLGA surface are represented only by terminal polymer groups, which are scarce even in the case of an acid-terminated low molecular weight polymer. One of the approaches to overcome these drawbacks is the use of PLGA NPs with functional hydrophilic shells, which, on the one hand, would protect the hydrophobic surface of NPs from opsonization and uptake by macrophages, and, on the other hand, would provide reactive groups for surface modification. Indeed, various types of core–shell PLGA NPs coated with shells composed of synthetic or natural polymers such as poloxamers, carbohydrates and proteins have proven to be effective for drug targeting and regenerative medicine.[4–8] Among these materials, human serum albumin (HSA) appears to be particularly attractive as a completely biocompatible and safe agent that not only provides various functional groups suitable for covalent attachment of ligands, but also prolongs blood circulation of NPs and improves drug targeting to tumors.[9–12]

Various approaches to the formation of the HSA shell on PLGA NPs have been described, such as interfacial embedding of HSA in the surface of NPs during their formation,[7] adsorption on preliminarily prepared PLGA NPs[10] or conjugation of HSA with terminal carboxyl groups of PLGA.[13–15] However, the quantitative parameters and stability of the PLGA/HSA core–shell system in a biological environment have not been sufficiently studied.

In this work, three different methods for the preparation of PLGA/HSA NPs were compared. The integrity of the systems was evaluated *in vitro* in the GL261 murine glioma cells.

All nanoparticles were prepared by multistep oil-in-water emulsification using a dichloromethane solution of acid-terminated PLGA and an aqueous solution of a surfactant (Scheme 1).[†] Interfacial embedding of HSA was achieved using an aqueous solution of HSA as the aqueous phase for the preparation of NPs. To form shells by adsorption, PLGA NPs were first prepared as described above with an aqueous solution of polyvinyl alcohol (PVA) as a stabilizer, and then HSA was allowed to adsorb onto PLGA NPs while incubating in the aqueous solution. The conjugation of amino groups of HSA with terminal carboxyl groups of PLGA (NPs were prepared as for adsorption) was carried out by the carbodiimide method.

[†] To prepare the nanoparticles, an acid-terminated PLGA, Purasorb® PDLG 5004A (Corbion Biomaterials), was used. The coarse emulsion obtained using an IKA UltraTurrax T18 disperser was further subjected to high-pressure emulsification with a Microfluidics M-110P homogenizer and solvent evaporation.

For interfacial embedding of HSA a 0.5% aqueous solution of HSA was used. After the formation of NPs, unbound HSA was removed by repeated washing and centrifugation of the nanosuspension (20 000 rpm, 20 °C, 20 min).

In the adsorption method, a 1% aqueous solution of PVA (9–10 kDa, 80% hydrolyzed, Merck) was used for emulsification. Then, free PVA was removed by centrifugation (20 000 rpm, 20 °C, 20 min), and the resulting PLGA NPs were incubated in a 0.5% aqueous solution of HSA at 37 °C for 30 min. Unbound HSA was removed by centrifugation as described above.

HSA was conjugated with PLGA by carbodiimide coupling (EDC, 1 h, 0.05 M phosphate buffer, pH 6.8).

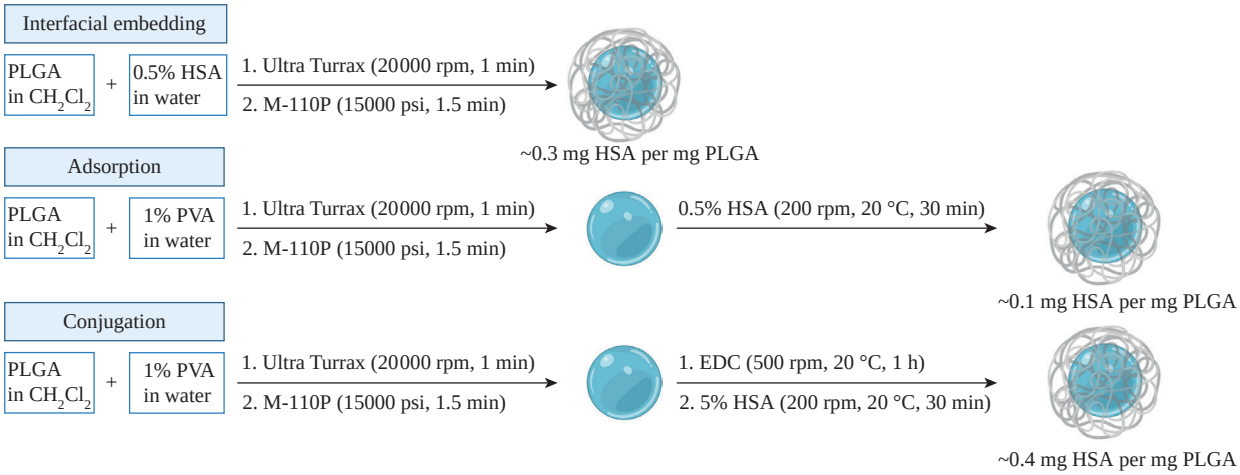

Scheme 1 PLGA/HSA nanoparticle preparation procedures.

Table 1 Physicochemical parameters of PLGA/HSA NPs prepared by different methods (representative data).

Method of HSA shell formation	Nanoparticle size		Volume size distribution		Zeta potential/mV	HSA content/ mg (mg PLGA)$^{-1}$
	Average size/nm	Polydispersity index	Peak size/nm	Volume (%)		
Interfacial embedding	132 ± 1	0.069 ± 0.014	130	100	−28.5 ± 0.6	0.3
Adsorption	136 ± 2	0.085 ± 0.046	134	100	−20.5 ± 1.2	0.1
HSA conjugation	149 ± 3	0.038 ± 0.017	152	100	−12.8 ± 0.4	0.4
NPs without shells	116 ± 2	0.098 ± 0.015	108	100	−20.9 ± 1.1	–
Cy5-PLGA/HSA-RhBITC interfacial embedding	102 ± 1	0.054 ± 0.030	97	100	−30.4 ± 2.6	0.3
Cy5-PLGA/HSA-RhBITC adsorption	131 ± 1	0.101 ± 0.016	129	100	−11.1 ± 2.6	0.1
Cy5-PLGA/HSA-RhBITC conjugation	140 ± 5	0.143 ± 0.039	138	100	−13.6 ± 2.0	0.4

The parameters of HSA-coated PLGA NPs are presented in Table 1.[‡] As can be seen, the coating of PLGA NPs with HSA led to an increase in their average diameter by 15–20 nm, with all NPs demonstrating negative zeta potentials (−20 mV on average). The less negative zeta potential of PLGA/HSA NPs obtained by HSA conjugation is due to the covalent bonding of –COOH groups on the surface of NPs with HSA amine groups.

Compared to the adsorption method, NPs prepared by the methods of interfacial embedding and conjugation have a higher content of albumin on the surface of NPs. For better stability in a biological environment, HSA shells on the surface of nanoparticles, prepared by the methods of interfacial embedding and conjugation, were additionally cross-linked with 8% glutaric aldehyde, as described previously.[17]

The stability of PLGA/HSA NPs prepared by different methods was evaluated by laser scanning confocal microscopy (LSCM)[§] using GL261 murine glioma cells (ATCC). For imaging of living cells, lasers with emission at 561 and 638 nm were used. Accordingly, to enable simultaneous visualization of both the polymer core and shell by LSCM, the nanoparticles were prepared using a PLGA conjugate with Cyanine5 dye (Cy5, λ_{ex} 651 nm, λ_{em} 670 nm, 1 : 1 mixture of conjugated and unmodified PLGA)[18] and HSA labeled with Rhodamine B isothiocyanate (RhBITC, λ_{ex} 543 nm, λ_{em} 580 nm). Accordingly, lasers emitting at 561 and 638 nm were used to image cells. To reveal the role of shell stability, we compared Cy5-PLGA/HSA-RhBITC double-labeled nanoparticles prepared by three methods (see Table 1). GL261 cells were incubated with nanoparticles and then examined with LSCM.[¶] To assess colocalization, the values of the Manders overlap coefficient were calculated.[19]

As can be seen from the images in Figure 1, NPs prepared by different methods are successfully internalized into cells, retaining their integrity. Accordingly, the values of the Manders overlap coefficients (Figure 2) in all cases exceeded 0.6, which also indicates colocalization of the labels.[19]

In conclusion, regardless of the preparation method, all PLGA/HSA systems retained their integrity when internalized into GL261 cells. The conjugation method makes it possible to obtain NPs with a high content of HSA on the NP surface, and the interfacial embedding of HSA appears to be a simple and convenient method for preparing PLGA NPs with an outer shell of HSA. The stability of the system makes PLGA/HSA NPs a reliable carrier for drug delivery to both extracellular and intracellular targets.

This work was carried out in accordance with the State Assignment of the Ministry of Science and Higher Education of the Russian Federation (project no. FSSM-2022-0003). The authors are grateful to the D. I. Mendeleev Center for the Collective Use of Scientific Equipment for performing analytical tests.

[‡] The average hydrodynamic diameter, polydispersity index and volume size distribution of PLGA/HSA NPs were determined by dynamic light scattering. The zeta potential was measured by electrophoretic light scattering using a Malvern Instruments Zetasizer Nano ZS particle analyzer.

The content of HSA in NPs was determined indirectly by the difference between the amount of added protein and the content of unbound protein measured by the colorimetric (biuret) method after separation of NPs.

For PLGA assay, the NPs were hydrolyzed in 1N NaOH solution, and then the lactic acid content was measured using a Lumex Kapel 105M capillary zonal electrophoresis system.[16]

[§] The images were taken using a Nikon A1R MP+ multiphoton confocal microscope.

[¶] GL261 cells cultured under standard conditions were incubated in confocal microscopy dishes (35 mm Ibidi coverslip/bottom confocal dishes) in RPMI culture medium supplemented with 10% fetal calf serum. After 24 h of cultivation, nanoparticles (final concentration 100 μg PLGA per ml) were added to the dishes and incubated for 30 min. After incubation, the cells were washed three times with PBS and then examined with LSCM.

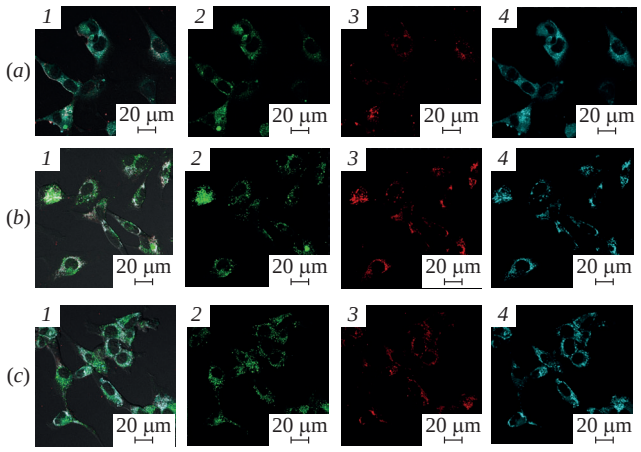

Figure 1 Intracellular distribution of Cy5-PLGA/HSA-RhBITC NPs, prepared by (*a*) interfacial embedding, (*b*) adsorption and (*c*) conjugation of HSA-RhBITC, after 30-min incubation with GL261 murine glioma cells: (*1*) combined image, (*2*) fluorescently labeled lysosomes (LysoTracker Green DND26 signal), (*3*) NPs internalized in cells (RhBITC signal) and (*4*) NPs internalized in cells (Cy5 signal).

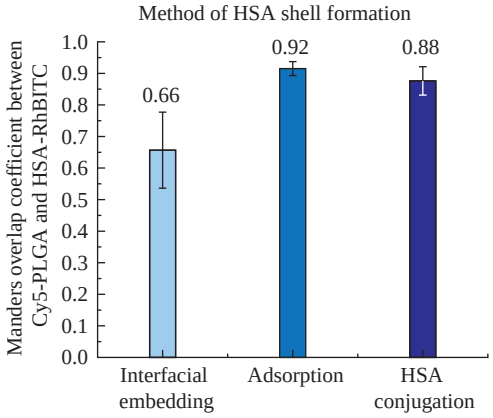

Figure 2 Manders overlap coefficients between Cy5 and RhBITC signals.

References

1 M. Mir, N. Ahmed and A. ur Rehman, *Colloids Surf., B*, 2017, **159**, 217.
2 E. V. Razuvaeva, K. T. Kalinin, N. G. Sedush, A. A. Nazarov, D. S. Volkov and S. N. Chvalun, *Mendeleev Commun.*, 2021, **31**, 512.
3 V. V. Sheffey, E. B. Siew, E. E. L. Tanner and O. Eniola-Adefeso, *Adv. Healthcare Mater.*, 2022, **11**, 2101536.
4 J. A. D. Sequeira, I. Pereira, A. J. Ribeiro, F. Veiga and A. C. Santos, in *Handbook of Functionalized Nanomaterials for Industrial Applications*, ed. C. M. Hussain, Elsevier, Amsterdam, 2020, pp. 185–203.
5 H. Chen, L. Q. Xie, J. Qin, Y. Jia, X. Cai, W. Nan, W. Yang, F. Lv and Q. Q. Zhang, *Colloids Surf., B*, 2016, **138**, 1.
6 T. U. Wani, S. N. Raza and N. A. Khan, *Polym. Bull.*, 2020, **77**, 3865.
7 S. Wohlfart, A. S. Khalansky, S. Gelperina, O. Maksimenko, C. Bernreuther, M. Glatzel and J. Kreuter, *PloS One*, 2011, **6**, e19121.
8 S. M. Kim, M. Patel and R. Patel, *Polymers*, 2021, **13**, 3471.
9 H. Tao, R. Wang, W. Sheng and Y. Zhen, *Int. J. Biol. Macromol.*, 2021, **187**, 24.
10 Q. Peng, S. Zhang, Q. Yang, T. Zhang, X.-Q. Wei, L. Jiang, C.-L. Zhang, Q.-M. Chen, Z.-R. Zhang and Y.-F. Lin, *Biomaterials*, 2013, **34**, 8521.
11 A. M. Merlot, D. S. Kalinowski and D. R. Richardson, *Frontiers in Physiology*, 2014, **5**, 299.
12 D. M. Dhoke, S. S. Basaiyye and P. B. Khedekar, *J. Drug Delivery Sci. Technol.*, 2018, **47**, 77.
13 S. Manoochehri, B. Darvishi, G. Kamalinia, M. Amini, M. Fallah, S. N. Ostad, F. Atyabi and R. Dinarvand, *Daru, J. Pharm. Sci.*, 2013, **21**, 58.
14 H. Hyun, J. Park, K. Willis, J. E. Park, L. T. Lyle, W. Lee and Y. Yeo, *Biomaterials*, 2018, **180**, 206.
15 P. Jiang, D. Yu, W. Zhang, Z. Mao and C. Gao, *RSC Adv.*, 2015, **5**, 40924.
16 Yu. Ermolenko, N. Nazarova, A. Belov, A. Kalistratova, Yu. Ulyanova, N. Osipova and S. Gelperina, *J. Drug Delivery Sci. Technol.*, 2022, **70**, 103220.
17 K. Langer, S. Balthasar, V. Vogel, N. Dinauer, H. von Briesen and D. Schubert, *Int. J. Pharm.*, 2003, **257**, 169.
18 Y. Malinovskaya, P. Melnikov, V. Baklaushev, A. Gabashvili, N. Osipova, S. Mantrov, Y. Ermolenko, O. Maksimenko, M. Gorshkova, V Balabanyan, J. Kreuter and S. Gelperina, *Int. J. Pharm.*, 2017, **524**, 77.
19 V. Zinchuk and O. Grossenbacher-Zinchuk, *Prog. Histochem. Cytochem.*, 2009, **44**, 125.

Received: 11th April 2023; Com. 23/7145